Am J Transl Res 2023;15(5):3267-3278
www.ajtr.org /ISSN:1943-8141/AJTR0148061

Original Article

Effect of susceptibility-weighted imaging on preoperative evaluation of microvascular decompression in patients with trigeminal neuralgia

Haipeng Xie[1*], Yingjie Zhang[2*], Yan Wang[1], Zetong Bai[1], Ziwei Zuo[3], Yanfang Shi[1], Xichao Wen[1], Kebin Zheng[1]

[1]Department of Neurosurgery, Affiliated Hospital of Hebei University, Baoding 071030, Hebei, The People's Republic of China; [2]Department of Rheumatology, Affiliated Hospital of Hebei University, Baoding 071030, Hebei, The People's Republic of China; [3]Department of Radiological, Affiliated Hospital of Hebei University, Baoding 071030, Hebei, The People's Republic of China. [*]Equal contributors.

Received November 27, 2022; Accepted April 9, 2023; Epub May 15, 2023; Published May 30, 2023

Abstract: Objective: To assess the effectiveness of susceptibility-weighted imaging (SWI) in displaying the superior petrosal vein complex (SPVC) and the role of venous three-dimensional (3D) reconstruction in visualizing the anatomical relationship in patients with trigeminal neuralgia (TN). Methods: A total of 30 patients with primary TN who received treatment between September 2019 and December 2020 were enrolled prospectively in this study. All patients were examined with fast imaging employing steady-state acquisition (Fiesta), three-dimensional time of flight (3D-TOF) and SWI by the same technician. Image analysis was performed by 2 physicians. 3D reconstruction of nerves, arteries, and veins was performed with 3dslicer and compared with intraoperative findings. The general characteristics, vein description in MRI, and the composition of SPVC types were also compared. Results: The display effect of SPVC in SWI was significantly better than that in Fiesta and 3D-TOF ($P < 0.05$). The display effect of phase images was found to be superior to magnitude images ($P < 0.05$). The superior petrosal vein, pontotrigeminal vein, transverse pontine vein, and vein of the cerebellopontine fissure were clearly displayed in SWI. The anatomical relationship between SPVC and trigeminal nerve shown by 3D reconstruction of the vein was consistent with the findings observed during the operation. Conclusion: The SPVC can be clearly displayed by SWI. 3D reconstruction of the vein can accurately display the anatomical relationship between the trigeminal nerve and SPVC.

Keywords: Trigeminal neuralgia, superior petrosal vein complex, three-dimensional reconstruction, preoperative evaluation

Introduction

Trigeminal neuralgia (TN) is a common disorder of the cranial nerve that is characterized by recurrent severe pain in the area of the trigeminal nerve distribution [1]. Microvascular decompression (MVD) is a well-accepted treatment method for TN [2]. While arterial compression is commonly recognized as the primary cause of TN, compression caused by the superior petrosal vein complex (SPVC) has also been widely observed during surgical interventions [3, 4]. Patients with TN who undergo MVD for venous compression tend to have a significantly lower cure rate and a higher recurrence rate compared to those without venous compression [5]. The superior petrosal vein (SPV) often interferes with the surgical approach during MVD [6]. The veins on the surface of the pons are more likely to compress the trigeminal nerve [7]. It is of critical importance to understand the structure of the vein around the trigeminal nerve so as to improve the curative efficacy of MVD. However, there is no detailed description of the SPVC based on magnetic resonance imaging (MRI).

Susceptibility-weighted imaging (SWI) is a technique that utilizes different magnetic susceptibility of tissues [8]. It is a high-resolution gradient echo sequence with three-dimensional (3D) acquisition and complete flow compensation [9]. SWI can display 100 μm venules and is widely used in the study of intracranial veins

Table 1. Sequence parameters of MRI scanning

Items	SWI	Fiesta	TOF
TR (ms)	37.8	3.78	11
TE (ms)	24.05	1.8	2.5
FOV (cm)	34.2×24	31.4×22	36.3×18
Slice thickness (mm)	0.8	0.8	0.7
Flip-angle (°)	15	55	15
AQM	256/320	192/160	256/192
THK	1.60	1.6	1.4

MRI, magnetic resonance imaging; TR, repetition time; TE, echo time; FOV, field of view; AQM, advanced quantitative metric; THK, thickness.

Table 2. Comparison of sensitivity of SPV in different display methods

Items	χ^2	*p* values
TOF vs. Fiesta*	32.03	< 0.005
Fiesta vs. Magnitude*	27.04	< 0.005
Fiesta vs. Phase*	27.04	< 0.005
Phase** vs. Magnitude	7.314	< 0.01
TOF vs. Phase*	59	< 0.005
TOF vs. Magnitude*	59	< 0.005

*has higher sensitivity in the comparison of SPV development rates between them. **has higher sensitivity in the comparison of SPV definition between them. SPV, superior petrosal vein; Fiesta, fast imaging employing steady-state acquisition; 3D-TOF, three-dimensional time of flight.

[10]. In this study, we compared the display rates of the SPV with its tributaries using SWI phase, SWI magnitude, fast imaging employing steady-state acquisition (Fiesta), and three-dimensional time of flight (3D-TOF) images. Moreover, we analyzed the types of SPVC and utilized a 3dslicer to reconstruct the nerves, arteries, and veins. Then, we compared these reconstructions with the intraoperative findings to assess their accuracy and consistency.

Subjects and methods

Subjects

The study was approved by the Ethics Committee of the Affiliated Hospital of Hebei University, and written informed consent was obtained from all participants. A total of 30 patients with TN who underwent MVD between September 2019 and December 2020 were included prospectively in this study. Inclusion criteria: (1) patients who aged over 18 years old; (2) patients who met the diagnostic criteria of TN [11]; (3) patients who had not received surgical treatment for trigeminal nerve lesions or craniotomy. Exclusion criteria: (1) patients who had cardiovascular or cerebrovascular diseases such as intracranial aneurysms, or cerebral and craniofacial arteriovenous malformations; (2) patients who had cognitive impairment; (3) patients who were not suitable for surgery due to severe diseases.

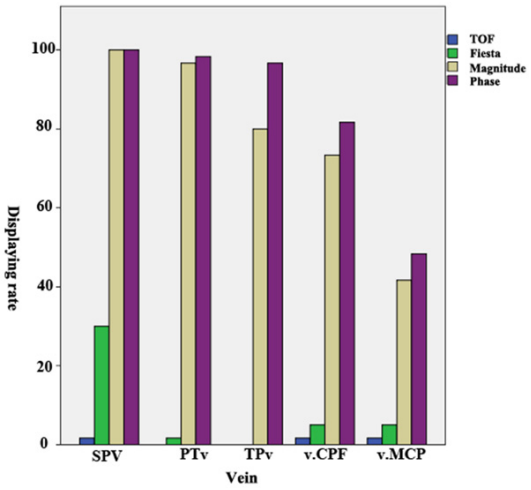

Figure 1. The display rate of each vein in TOF, Fiesta, Magnitude and Phase. Fiesta, fast imaging employing steady-state acquisition; 3D-TOF, three-dimensional time of flight.

MRI scan

All patients underwent imaging examinations using fast imaging employing steady-state acquisition (Fiesta), 3D-TOF-MRA, and SWI, performed by the same trained technician. A GE Discovery MR 750 3.0T scanner (Milwaukee, WI, USA) was used. The patients were positioned in the standard anatomic supine position on the MRI table, with an 8-channel phased array head coil placed on the head. The scanning plane was parallel to the anterior-posterior joint plane to ensure symmetry of the anatomic structure. The sequence parameters are detailed in **Table 1**. Volume viewer software was used for image post-processing.

Vein description

The MRI images of all subjects were analyzed independently by two neurosurgeons. The SPV, pontotrigeminal vein (PTv), transverse pontine

Table 3. Comparison of display rate of each vein in TOF, Fiesta, magnitude and phase

Items		Quality of the vein depiction						χ^2	*P* values
		Not identified		Identified		Identified clearly			
		N	%	N	%	N	%		
SPV	Fiesta	42	70.00	13	21.67	5	8.33	227.533	< 0.001
	Magnitude	0	.00	34	56.67	26	43.33		
	Phase	0	.00	9	15.00	51	85.00		
	TOF	59	98.33	1	1.67	0	0.00		
PTv	Fiesta	59	98.33	1	1.67	0	0.00	241.108	< 0.001
	Magnitude	2	3.33	21	35.00	37	61.67		
	Phase	1	1.67	7	11.67	52	86.67		
	TOF	60	100.00	0	0.00	0	0.00		
TPv	Fiesta	60	100.00	0	0.00	0	.00	231.301	< 0.001
	Magnitude	12	20.00	29	48.33	19	31.67		
	Phase	2	3.33	11	18.33	47	78.33		
	TOF	60	100.00	0	0.00	0	0.00		
v.CPF	Fiesta	57	95.00	2	3.33	1	1.67	160.552	< 0.001
	Magnitude	16	26.67	24	40.00	20	33.33		
	Phase	11	18.33	10	16.67	39	65.00		
	TOF	59	98.33	1	1.67	0	.00		
v.MCP	Fiesta	57	95.00	2	3.33	1	1.67	64.623	< 0.001
	Magnitude	35	58.33	12	20.00	13	21.67		
	Phase	31	51.67	7	11.67	22	36.67		
	TOF	59	98.33	1	1.67	0	.00		

SPVC, superior petrosal vein complex; SPV, superior petrosal vein; PTv, pontotrigeminal vein; TPv, transverse pontine vein; v.CPF, vein of the cerebellopontine fissure; v.MCP, vein of the middle cerebellar peduncle; Fiesta, fast imaging employing steady-state acquisition; 3D-TOF, three-dimensional time of flight.

vein (TPv), vein of the cerebellopontine fissure (v.CPF), and vein of the middle cerebellar peduncle (v.MCP) were identified in SWI phase, SWI magnitude, Fiesta, and TOF-MRA images. We described SPVC based on the SWI phase and SWI magnitude images. The description contained the number of SPVs, the composition of SPVC, and the type of SPV discharged into the sensory processing sensitivity (SPS).

Neuroarteriovenous reconstruction

Medical digital imaging and communication (DICOM) of all subjects were imported into 3dslicer software (3dslicer 4.11), preoperatively. 3D reconstruction of the brainstem, cranial nerve, artery, and SPVC was performed by the same senior neurosurgery attending physician.

Operative technique

All procedures were performed via the retrosigmoid approach by the same chief neurosurgeon. The trigeminal nerve and peripheral vessels were exposed. The SPVC was carefully observed in operation. We observed the anatomical relationship between the trigeminal nerve and SPVC from different angles. Teflon was filled between trigeminal nerve and the offending vessel to suture the dura mater. We considered the intraoperative findings as the definitive criterion for determining the relationship between the vein and trigeminal nerve.

Outcome indexes

The general characteristics, vein description in MRI, and the composition of SPVC types were compared.

Statistical analysis

All statistical analyses were performed using IBM SPSS Statistics for Windows (version 24.0; IBM Corp). The comparison of the performances of different imaging methods was carried out by the 3-dimensional paired chi-squared test. The measurement data were compared by

Table 4. Comparison of standardized residuals in TOF, Fiesta, magnitude and phase after adjustment by post hoc testing

Items		Quality of the vein depiction			Cramer's V	*P* values
		Not identified	Identified	Identified clearly		
SPV	TOF	10.2	-4.6	-6.4	0.688	< 0.001
	Fiesta	5.1	-.4	-4.9		
	Magnitude	-7.6	6.9	1.7		
	Phase	-7.6	-1.8	9.6		
PTv	TOF	8.8	-3.3	-6.9	0.712	< 0.001
	Fiesta	8.5	-2.9	-6.9		
	Magnitude	-8.5	6.3	4.6		
	Phase	-8.8	-.1	9.2		
TPv	TOF	8.0	-4.0	-5.5	0.694	< 0.001
	Fiesta	8.0	-4.0	-5.5		
	Magnitude	-6.5	7.6	.8		
	Phase	-9.5	.4	10.2		
v.CPF	TOF	7.1	-3.4	-5.2	0.578	< 0.001
	Fiesta	6.5	-3.0	-4.8		
	Magnitude	-6.0	6.1	1.7		
	Phase	-7.5	.3	8.3		
v.MCP	TOF	4.7	-2.3	-3.8	0.367	< 0.001
	Fiesta	4.0	-1.8	-3.3		
	Magnitude	-3.7	3.4	1.7		
	Phase	-5.0	.8	5.4		

SPV, superior petrosal vein; PTv, pontotrigeminal vein; TPv, transverse pontine vein; v.CPF, vein of the cerebellopontine fissure; v.MCP, vein of the middle cerebellar peduncle; Fiesta, fast imaging employing steady-state acquisition; 3D-TOF, three-dimensional time of flight.

t-test. The categorical data of the patients were assessed by chi-square tests. $P < 0.05$ was considered statistically significant (two-sided).

Results

General characteristics

Among the 30 patients with TN, there were 15 males and 15 females, with an average age of (45.3 ± 10.27) years old. Their average medical history was (7.1 ± 5.2) years. There were 12 patients with pain involving one branch and 18 patients with pain involving two or three branches of the trigeminal nerve. Moreover, there were 13 patients with pain on the right side, and 17 on the left side.

SPV was found in all patients during surgery. The sensitivity of TOF, Fiesta, Magnitude and Phase to SPV display was compared (**Table 2**). Compared with TOF, Phase and Magnitude imaging techniques demonstrated higher sensitivity (1.67% vs. 100%, $P < 0.005$). Compared with Fiesta, Phase and Magnitude exhibited higher sensitivity (30% vs. 100%, $P < 0.005$). We compared the clarity of SPV display between Phase and Magnitude, and the results showed that Phase exhibited higher sensitivity than Magnitude (43.3% vs. 85%, $P < 0.01$).

Vein description in MRI

There were significant differences in the display rate of the SPVC veins on MRI, with the display effect of veins classified into three grades: not identified, identified, and clearly identified. The display rate was calculated by summing the proportions of clearly identified and identified veins. The display rate of the SPV was 100% in both magnitude and phase images but was only 30% in the Fiesta images. The SPV was recognized during TOF angiography. The display rate of the PTv was 96.67% and 98.33% in the magnitude and phase images, respectively. However, the PTv was not recognized in Fiesta images and during TOF angiography. The dis-

Table 5. Comparison of displaying rate of SPv, PTv, TPv, v.CPF and v.MCP in different display methods

Items		Quality of the vein depiction						χ^2	*P* values
		Not identified		Identified		Identified clearly			
		N	%	N	%	N	%		
Fiesta	SPV	42	70.00	13	21.67	5	8.33	47.694	< 0.001
	PTv	59	98.33	1	1.67	0	.00		
	TPv	60	100.00	0	.00	0	.00		
	v.CPF	57	95.00	2	3.33	1	1.67		
	v.MCP	57	95.00	2	3.33	1	1.67		
Magnitude	SPV	0	.00	34	56.67	26	43.33	86.239	< 0.001
	PTv	2	3.33	21	35.00	37	61.67		
	TPv	12	20.00	29	48.33	19	31.67		
	v.CPF	16	26.67	24	40.00	20	33.33		
	v.MCP	35	58.33	12	20.00	13	21.67		
Phase	SPV	0	.00	9	15.00	51	85.00	91.801	< 0.001
	PTv	1	1.67	7	11.67	52	86.67		
	TPv	2	3.33	11	18.33	47	78.33		
	v.CPF	11	18.33	10	16.67	39	65.00		
	v.MCP	31	51.67	7	11.67	22	36.67		
TOF	SPV	59	98.33	1	1.67	0	.00	2.020	0.732
	PTv	60	100.00	0	.00	0	.00		
	TPv	60	100.00	0	.00	0	.00		
	v.CPF	59	98.33	1	1.67	0	.00		
	v.MCP	59	98.33	1	1.67	0	.00		

SPV, superior petrosal vein; PTv, pontotrigeminal vein; TPv, transverse pontine vein; v.CPF, vein of the cerebellopontine fissure; v.MCP, vein of the middle cerebellar peduncle; Fiesta, fast imaging employing steady-state acquisition; 3D-TOF, three-dimensional time of flight.

play rate of the TPv in the magnitude and phase images was 80% and 96.67%, respectively. Nevertheless, the TPv was not recognized in the Fiesta images and during TOF angiography. The display rate of v.CPF in the magnitude and phase images was 73.33% and 81.67%, respectively. Occasionally, the cisternal segment of the v.CPF was detected in Fiesta and TOF images. The display rate of the v.MCP in the magnitude and phase images was 41.67% and 48.33%, respectively. In some cases, the cisternal segment of the v.MCP was detected in Fiesta and TOF images (**Figure 1**). The display rates of each vein within the SPVC were notably different in the TOF, Fiesta, SWI magnitude, and SWI phase images (**Table 3**).

The absolute values of standardized residuals of the quality of vein depiction in the phase images of the SPVC were 9.6, 9.2, 10.2, 8.3, and 5.4. Therefore, the phase images clearly showed the venous branches of the SPVC (**Table 4**). The quality of the venous depiction had a significant difference from the development method. Compared with Fiesta and TOF images, phase images had a better description quality for the SPVC. Although phase images clearly displayed the SPV, PTv, TPv, and v.CPF, the v.MCP had a low display probability.

There was a correlation between vein types and the quality of vein depiction in Fiesta, magnitude, and phase images (**Table 5**). Moreover, the correlation between magnitude images and vein types was the strongest, while that in the Fiesta images was the weakest (**Table 6**). This finding showed that while magnitude images provided clear visualization of the veins, they were susceptible to interference from the anatomic position of the vein, resulting in significant variability in image quality among different veins. Phase images demonstrated clear visualization of each vein and were less susceptible to interference from the anatomic position of the vein. The adjusted standardized residuals of the undeveloped rate of the v.MCP in the magnitude and phase images were 7.7 and 8.9, respectively. Compared with other veins in the

Table 6. Comparison of standardized residuals of SPV, PTv, TPv, v.CPF and v.MCP in different developing methods after post hoc testing

Items		Quality of the vein depiction			Cramer's V	*P* values
		Not identified	Identified	Identified clearly		
TOF	SPV	-0.6	0.6	0.0	0.082	0.732
	PTv	0.9	-0.9	0.0		
	TPv	0.9	-0.9	0.0		
	v.CPF	0-.6	0.6	0.0		
	v.MCP	-0.6	0.6	0.0		
Fiesta	SPV	-6.8	5.7	3.4	0.282	< 0.001
	PTv	2.1	-1.6	-1.3		
	TPv	2.6	-2.2	-1.3		
	v.CPF	1.0	-1.0	-0.4		
	v.MCP	1.0	-1.0	-0.4		
Magnitude	SPV	-4.6	2.9	0.9	0.694	< 0.001
	PTv	-3.9	-0.9	4.2		
	TPv	-0.4	1.5	-1.2		
	v.CPF	1.1	0.0	-0.9		
	v.MCP	7.7	-3.5	-3.0		
Phase	SPV	-3.6	0.1	2.8	0.578	< 0.001
	PTv	-3.2	-0.7	3.1		
	TPv	-2.8	0.9	1.5		
	v.CPF	0.8	0.5	-1.0		
	v.MCP	8.9	-0.7	-6.4		

SPV, superior petrosal vein; PTv, pontotrigeminal vein; TPv, transverse pontine vein; v.CPF, vein of the cerebellopontine fissure; v.MCP, vein of the middle cerebellar peduncle; Fiesta, fast imaging employing steady-state acquisition; 3D-TOF, three-dimensional time of flight.

SPVC, the MCP had a lower development rate and image quality. Fiesta images showed part of the SPV, but they did not identify the branches (**Figure 2**).

The vein description

Among 60 sides of the SPVC in all 30 patients, one SPV was identified on 56 sides, while two SPVs were observed on four sides. We did not identify patients with three SPVs (**Figure 3**). According to Basamh et al., the drainage types of the SPV were classified into three categories based on the location of SPV flow into the SPS, including type I (lateral drainage), type II (intermediate drainage) and type III (medial drainage). There were 64 SPVs on 60 sides of the 30 patients, including 2 type I veins, 9 type II veins, and 53 type III veins (**Figure 4**).

Composition of SPVC types

There were 17 SPVC types in 30 patients. The three most common types were PTv+TPv+v.CPF, PTv+v.CPF+v.MCP and PTv+TPv (**Table 7**). The impact of SPVC on surgery was classified into the following 3 categories: 1. disturbed, which referred to the exposure of the trigeminal nerve and REZ area by vein interference, requiring free displacement of the vein to fully display the trigeminal nerve and REZ area; 2. compressed, while referred to compression of the trigeminal nerve and REZ area by the vein alone or together with the artery; and 3. non-disturbed, which meant that the trigeminal nerve and REZ area were clearly displayed without treatment of the vein. The images of 3D reconstruction showed that the SPVC did not interfere with the MVD in 25 cases. The SPVC branches of 3 patients interfered with the operative field. The SPV and TPv were identified as the offending vein in one case each. The coincidence rate of 3D reconstruction results and intraoperative exploration results was 100% (**Table 8**; **Figure 5**).

Discussion

At present, some scholars have used SWI to explain the venous network around the brain

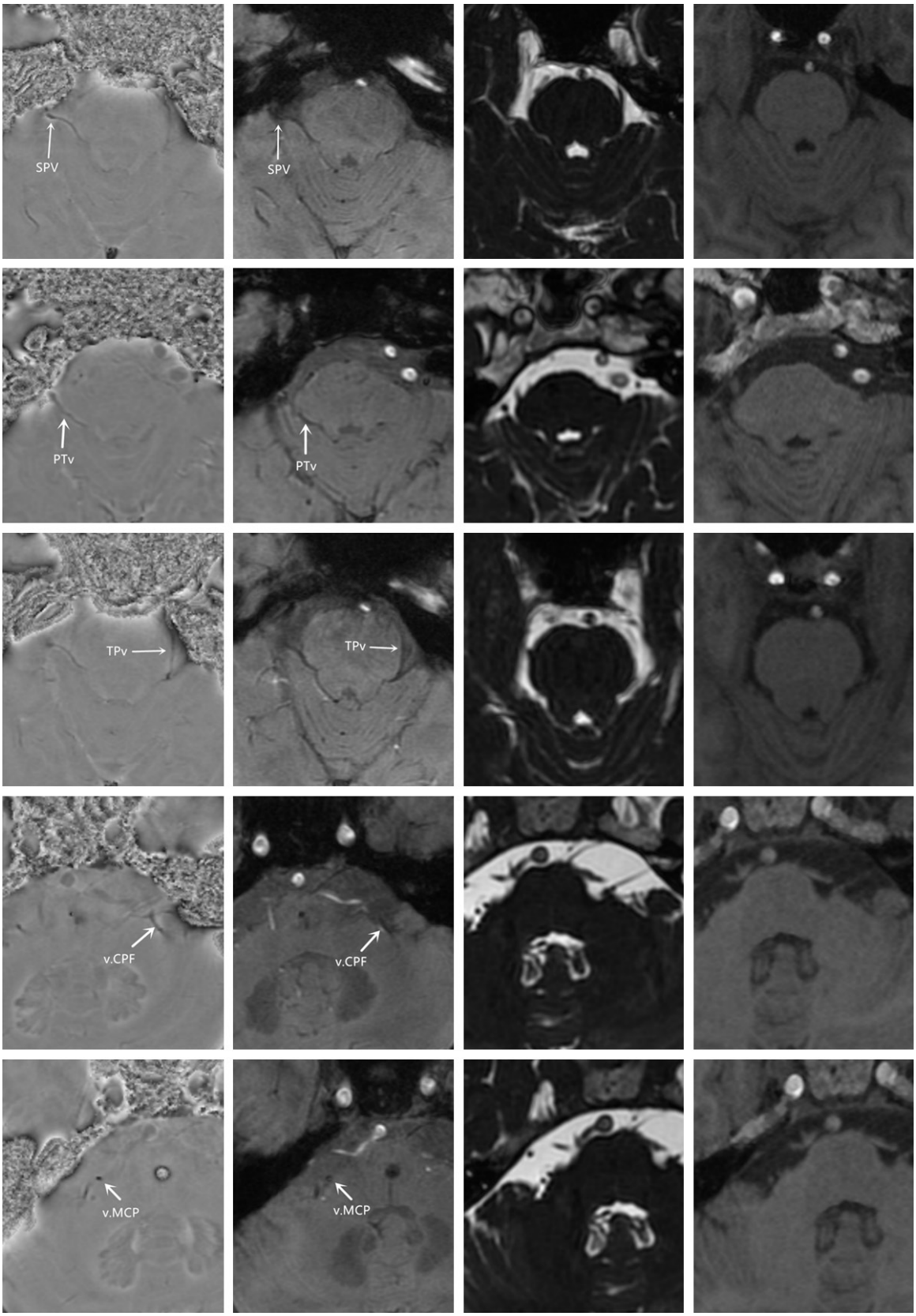

Figure 2. The display effect of SPVC in SWI was better than that in Fiesta and TOF. SWI, susceptibility-weighted imaging; SPVC, superior petrosal vein complex; 3D-TOF, three-dimensional time of flight; Fiesta, fast imaging employing steady-state acquisition; SPV, superior petrosal vein; PTv, pontotrigeminal vein; TPv, transverse pontine vein; v.CPF, a vein of the cerebellopontine fissure; v.MCP, a vein of the middle cerebellar peduncle.

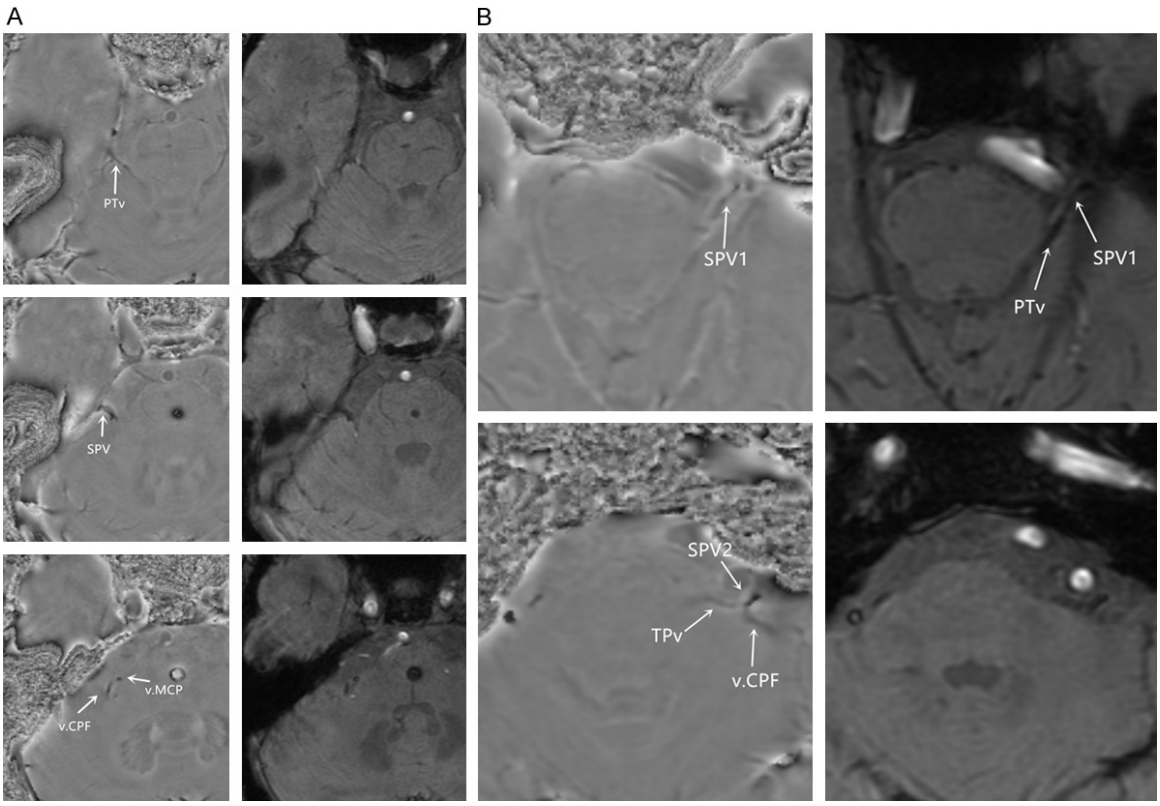

Figure 3. The imaging of the patients with SPV. A. A patient with one single SPV on the right side, whose branches included PTv, v.CPF and v.MCP. B. A patient with two SPVs on the left side. The first SPV has only one branch of PTv. The second SPV is composed of TPv and v.CPF. SPV, superior petrosal vein; PTv, pontotrigeminal vein; TPv, transverse pontine vein; v.CPF, a vein of the cerebellopontine fissure; v.MCP, a vein of the middle cerebellar peduncle.

stem [12]. However, due to the special anatomic position of the SPVC, the SWI images were affected by the tail shadow of the bone signal. The display rate was still low, and interference from arteries further affected the visibility of the veins on SWI images. Therefore, the vein position information can be lost during SWI compression imaging. In the past, the importance of SWI magnitude and phase images may have been overlooked. These two types of images not only contain vein position information but also enable identification of the SPV and its branches in phase images. They have a high display rate and high definition for PTv and TPv. Clear visualization of these two veins is very important. PTv injury has been associated with a potential risk of midbrain hemorrhage [13]. TPv is the most common offending vein [7, 14]. In the current study, the display rate of the MCP was still low. However, there are few reports on the involvement of MCP in the cranial nerve and its interference with the operative field. In the current study, the majority of the patients had one SPV, and drainage pattern of the SPV was type III, which differs from the findings of previous studies and requires confirmation based on a large number of cases.

At present, many anatomic and intraoperative studies have described the composition of SPVC in detail [15-17]. We described 17 types of venous combinations, and there are no other studies that have provided similar descriptions. The PTv and TPv are the most common primary branches of the SPVC, and the MCP is the most common secondary branch. When the SPV is not involved in the formation of the SPVC, the SPV often anastomoses with the basilar and Galen veins. Although the TPv rarely extends to the contralateral side, the TPv is often anastomosed with the longitudinal vein anterior to the pons. The v.CPF often anastomoses with the vPon., Med., Sulc and inferior petrosal vein. These different types of veins and types of communication between veins is likely to play a key role on the outcomes of SPV amputation.

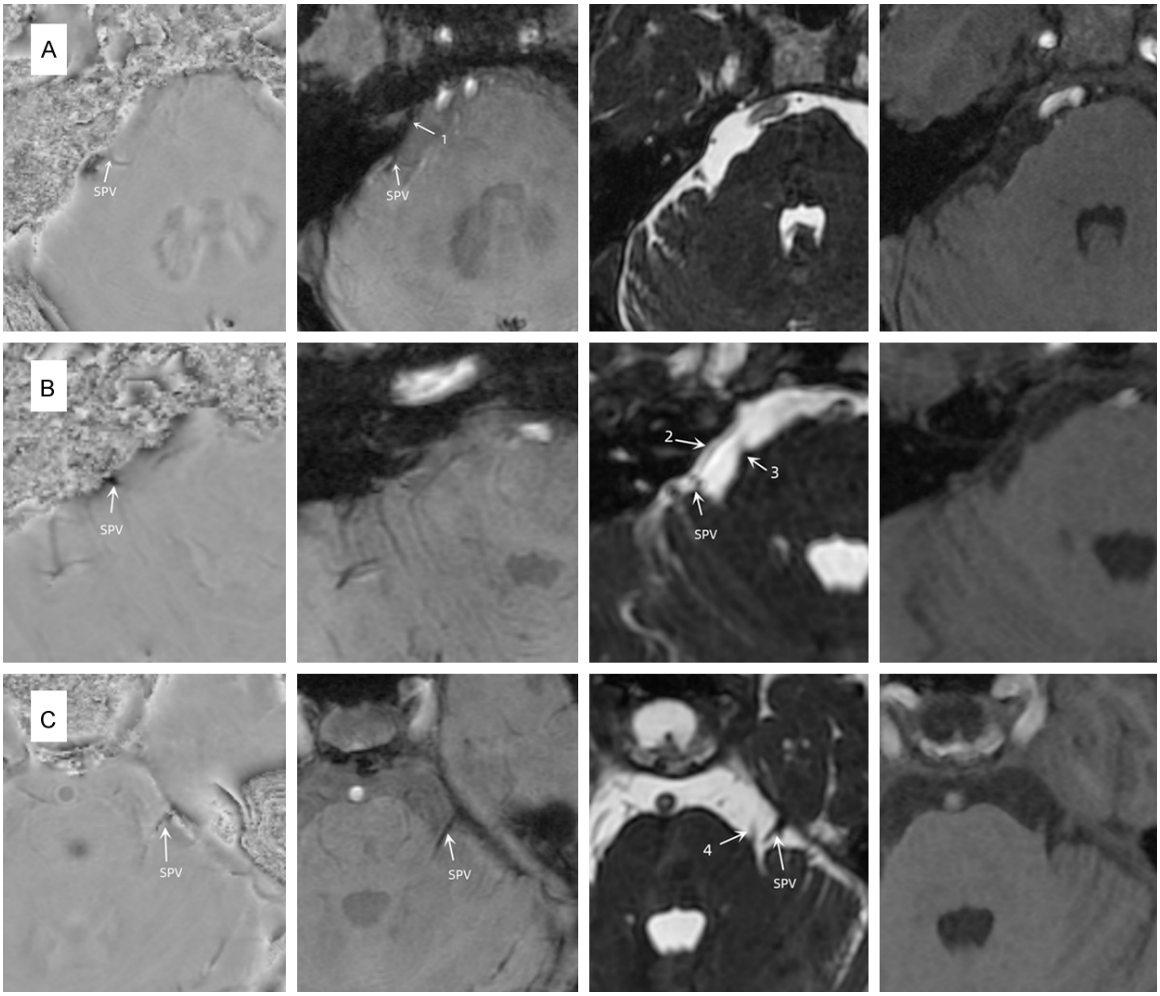

Figure 4. Type of SPV drainage into the SPS. A. Type I drainage of the SPV into the SPS; B. Type II drainage of the SPV into the SPS; C. Type III drainage of the SPV into the SPS. 1: Internal auditory canal; 2: Superior margin of internal auditory canal; 3: Inferior margin of trigeminal nerve; 4: Superior margin of trigeminal nerve. SPV, superior petrosal vein; SPS, sensory processing sensitivity.

Simplifying the classification and aligning it with surgical techniques will be a focus of further research in our center.

Currently, some scholars have summarized the surgical effect of TN caused by venous compression [3, 4]. The proportion of venous compression in the current study was 6.67%, which is consistent with a previous study. The SPV interfered with the operative field in 54% of the patients [7]. There is ongoing debate regarding whether the vein directly compresses the trigeminal nerve and whether the vein that interferes with the surgical approach can be safely cut off. Many studies have reported conflicting results on this topic. Some scholars have suggested that surgical removal of the SPV does not significantly impact patients, while others have argued that such intervention can result in severe consequences [14, 18-25]. These controversies highlight the importance of the preoperative evaluation of the SPVC.

Although the effect of 3D reconstruction on identifying the responsible artery of TN has been confirmed, there are few studies on the relationship between the SPVC and trigeminal nerve position. A small number of studies have investigated the relationship between the SPV and trigeminal nerve by 3D reconstruction, but all of the studies used the vascular flow void effect in T2 or Fiesta images to determine the location of the SPV cistern segment [26]. The results of our study showed that the phase

Table 7. The types of branches of superior petrosal vein

Types	Amount
PTV+TPV+v.CPF	16
TPV+MCP+v.CPF	2
PTV	4
(TPV-MCP)+v.CPF	1
PTV+v.CPF+MCP	7
PTV+(TPV-MCP)+v.CPF	4
PTV+TPV	7
MCP+v.CPF	5
PTV+(TPV-v.CPF)	1
PTV+(TPV-MCP)	3
PTV+TPV+MCP+v.CPF	4
PTV+MCP	1
PTV+v.CPF+(MCP-TPV)	2
TPV+v.CPF	3
PTV+TPV+MCP	1
PTV+v.CPF	2
TPV+MCP	1
Total	64

A+B+C means that A, B and C are the first-order branches of SPV. D+(E-F) means that D and E are the first-order branches of SPV, and F flows into E. SPV, superior petrosal vein; PTv, pontotrigeminal vein; TPv, transverse pontine vein; v.CPF, vein of the cerebellopontine fissure; v.MCP, vein of the middle cerebellar peduncle.

images were superior to Fiesta images in terms of display rate and depicting the effect of the SPVC. The uncompressed phase images contain the position information of the vein. In the current study, 3D reconstruction of the SPVC was performed on phase images, and the results were consistent with the intraoperative findings. Based on 3D reconstruction, we can understand the types of SPVC branches and venous communication, and identify veins beyond the limitations of the surgical field. Although in this study, there was no need to cut off the SPV or its branches, we believe that the SPV containing the TPv and v.CPF can be cut off if necessary, as these two veins often have abundant anastomoses. However, caution should be exercised when the PTv is the only branch of the SPV, as cutting off the SPV may be risky due to the usual lack of a venous anastomosis in the SPV.

This study also has some limitations. First of all, the sample size is too small. Secondly, the interference of human factors on the results was not excluded. Thirdly, we did not include surgeon satisfaction as an evaluation index. Future studies should increase the sample size and reduce the bias caused by human factors.

Table 8. The coincidence rate of 3D reconstruction and intraoperative exploration

Sex	Side	VR-NVR	MVD-NVR
M	R	Offend (SPV)	Offend (SPV)
F	R	non-disturb	non-disturb
M	R	disturb (tributary)	disturb (tributary)
M	L	disturb (tributary)	disturb (tributary)
M	R	non-disturb	non-disturb
F	R	non-disturb	non-disturb
M	R	non-disturb	non-disturb
F	L	non-disturb	non-disturb
F	R	non-disturb	non-disturb
F	R	non-disturb	non-disturb
F	R	non-disturb	non-disturb
F	L	non-disturb	non-disturb
F	L	non-disturb	non-disturb
M	R	non-disturb	non-disturb
M	L	non-disturb	non-disturb
M	L	non-disturb	non-disturb
M	R	non-disturb	non-disturb
M	R	non-disturb	non-disturb
M	L	disturb (tributary)	disturb (tributary)
M	L	non-disturb	non-disturb
M	R	Offend (TPV)	Offend (TPV)
M	R	non-disturb	non-disturb
F	R	non-disturb	non-disturb
F	L	non-disturb	non-disturb
F	R	non-disturb	non-disturb
F	R	non-disturb	non-disturb
F	R	non-disturb	non-disturb
F	L	non-disturb	non-disturb
F	L	non-disturb	non-disturb
M	R	non-disturb	non-disturb

M, male; F, female; R, right; L, left. VR-NVR, Virtual Reality - Network video recorder; MVD-NVR, Microwave Video Distribution - Network video recorder; SPV, superior petrosal vein; TPv, transverse pontine vein.

Conclusion

In conclusion, the SPVC can be clearly displayed by SWI. 3D reconstruction of the vein can accurately display the anatomical relationship between the trigeminal nerve and SPVC.

Disclosure of conflict of interest

None.

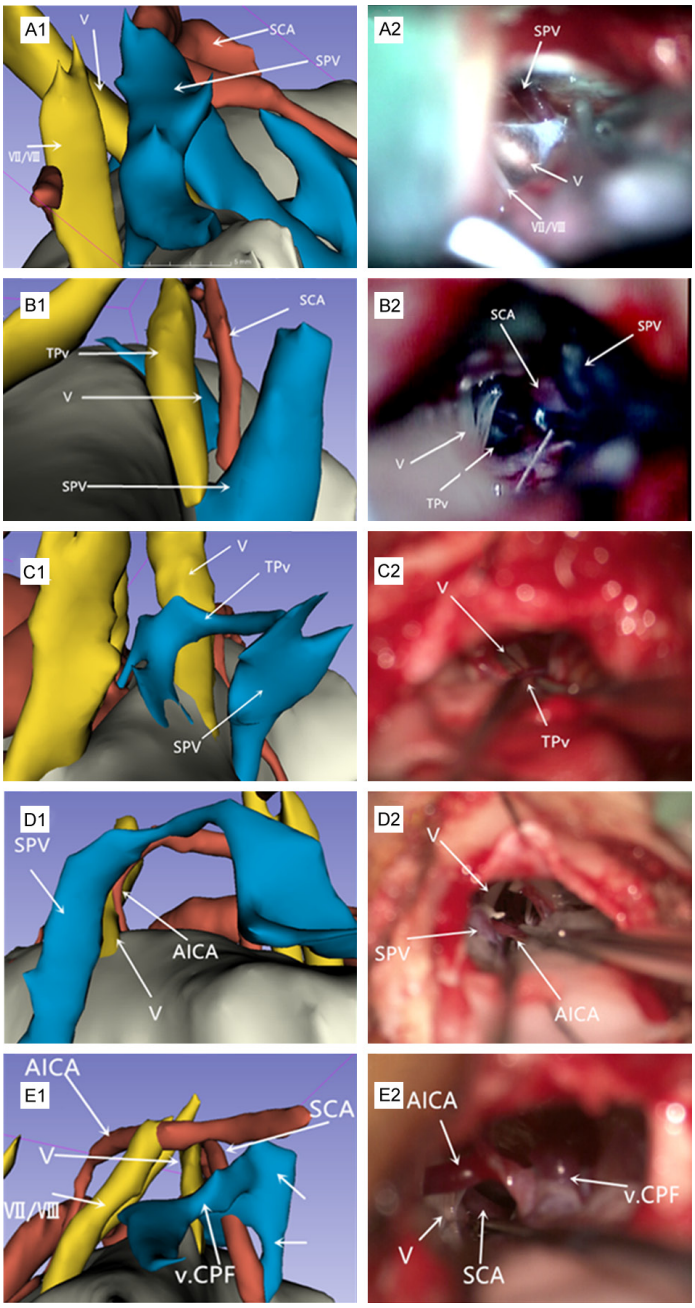

Figure 5. Imaging of 3D reconstruction. A1. 3D reconstruction showed that the SPV was located above the trigeminal nerve. A2. The relationship between the vein and trigeminal nerve in three-dimensional reconstruction was consistent with that in operation. B1. 3D reconstruction showed that the trigeminal nerve was compressed by TPv. B2. The intraoperative findings were consistent with the results of 3D reconstruction. C1. 3D reconstruction results showed that TPv interfered with the operation field. C2. Intraoperative findings. D1. 3D reconstruction showed that SPV was located above the trigeminal nerve and did not interfere with the operation site. D2. There is no need to disturb SPV during operation. E1. 3D reconstruction results showed that v.CPF interfered with the operation field. E2. During the operation, the v.CPF should be shifted to show the responsible vessels. 3D reconstruction, three-dimensional reconstruction; SPV, superior petrosal vein; CPF, erebellopontine fissure; TPv, transverse pontine vein.

Address correspondence to: Kebin Zheng, Department of Neurosurgery, Affiliated Hospital of Hebei University, No. 212 Yuhua Avenue, Baoding 071030, Hebei, The People's Republic of China. Tel: +86-0312-5981818; E-mail: zhengkebinzkb@163.com

References

[1] Maarbjerg S, Di Stefano G, Bendtsen L and Cruccu G. Trigeminal neuralgia - diagnosis and treatment. Cephalalgia 2017; 37: 648-657.

[2] Zhang WB, Zeng YY, Chang BW, Min LZ, Sun QY, Bin Li, Tao BB and Wang XQ. Prognostic nomogram for microvascular decompression-treated trigeminal neuralgia. Neurosurg Rev 2021; 44: 571-577.

[3] Toda H, Iwasaki K, Yoshimoto N, Miki Y, Hashikata H, Goto M and Nishida N. Bridging veins and veins of the brainstem in microvascular decompression surgery for trigeminal neuralgia and hemifacial spasm. Neurosurg Focus 2018; 45: E2.

[4] Akkaya E, Gokcil Z, Erbas C, Pusat S, Bengisun ZK and Erdogan E. A clinical analysis of microvascular decompression surgery with sacrification of the superior petrosal venous complex for trigeminal neuralgia: a single-surgeon experience. Turk Neurosurg 2020; 30: 83-88.

[5] Wu M, Fu X, Ji Y, Ding W, Deng D, Wang Y, Jiang X and Niu C. Microvascular decompression for classical trigeminal neuralgia caused by venous compression: novel anatomic classifications and surgical strategy. World Neurosurg 2018; 113: e707-e713.

[6] Liebelt BD, Barber SM, Desai VR, Harper R, Zhang J, Parrish R, Baskin DS, Trask T and Britz GW. Superior petrosal vein sacrifice during microvascular decompression: perioperative complication rates and comparison with venous preservation. World Neurosurg 2017; 104: 788-794.

[7] Basamh M, Sinning N and Kehler U. Individual variations of the superior petrosal vein complex and their microsurgical relevance in 50 cases of trigeminal microvascular

decompression. Acta Neurochir (Wien) 2020; 162: 197-209.
[8] Liu C, Li W, Tong KA, Yeom KW and Kuzminski S. Susceptibility-weighted imaging and quantitative susceptibility mapping in the brain. J Magn Reson Imaging 2015; 42: 23-41.
[9] Liu S, Buch S, Chen Y, Choi HS, Dai Y, Habib C, Hu J, Jung JY, Luo Y, Utriainen D, Wang M, Wu D, Xia S and Haacke EM. Susceptibility-weighted imaging: current status and future directions. NMR Biomed 2017; 30: 10.1002/nbm.3552.
[10] Sehgal V, Delproposto Z, Haacke EM, Tong KA, Wycliffe N, Kido DK, Xu Y, Neelavalli J, Haddar D and Reichenbach JR. Clinical applications of neuroimaging with susceptibility-weighted imaging. J Magn Reson Imaging 2005; 22: 439-450.
[11] Brinzeu A, Dumot C and Sindou M. Role of the petrous ridge and angulation of the trigeminal nerve in the pathogenesis of trigeminal neuralgia, with implications for microvascular decompression. Acta Neurochir (Wien) 2018; 160: 971-976.
[12] Cai M, Zhang XF, Qiao HH, Lin ZX, Ren CG, Li JC, Chen CC and Zhang N. Susceptibility-weighted imaging of the venous networks around the brain stem. Neuroradiology 2015; 57: 163-169.
[13] Ebner FH, Roser F, Shiozawa T, Ruetschlin S, Kirschniak A, Koerbel A and Tatagiba M. Petrosal vein occlusion in cerebello-pontine angle tumour surgery: an anatomical study of alternative draining pathways. Eur J Surg Oncol 2009; 35: 552-6.
[14] Anichini G, Iqbal M, Rafiq NM, Ironside JW and Kamel M. Sacrificing the superior petrosal vein during microvascular decompression. Is it safe? Learning the hard way. Case report and review of literature. Surg Neurol Int 2016; 7 Suppl 14: S415-S420.
[15] Matsushima T, Rhoton AL Jr, de Oliveira E and Peace D. Microsurgical anatomy of the veins of the posterior fossa. J Neurosurg 1983; 59: 63-105.
[16] Matsushima K, Matsushima T, Kuga Y, Kodama Y, Inoue K, Ohnishi H and Rhoton AL Jr. Classification of the superior petrosal veins and sinus based on drainage pattern. Neurosurgery 2014; 10 Suppl 2: 357-367.
[17] Rhoton AL Jr. The posterior fossa veins. Neurosurgery 2000; 47 Suppl: S69-S92.
[18] Pathmanaban ON, O'Brien F, Al-Tamimi YZ, Hammerbeck-Ward CL, Rutherford SA and King AT. Safety of superior petrosal vein sacrifice during microvascular decompression of the trigeminal nerve. World Neurosurg 2017; 103: 84-87.
[19] Xia Y, Kim TY, Mashouf LA, Patel KK, Xu R, Casaos J, Choi J, Kim ES, Hung AL, Wu A, Garzon-Muvdi T, Bender MT, Jackson CM, Bettegowda C and Lim M. Absence of ischemic injury after sacrificing the superior petrosal vein during microvascular decompression. Oper Neurosurg (Hagerstown) 2020; 18: 316-320.
[20] Hong W, Zheng X, Wu Z, Li X, Wang X, Li Y, Zhang W, Zhong J, Hua X and Li S. Clinical features and surgical treatment of trigeminal neuralgia caused solely by venous compression. Acta Neurochir (Wien) 2011; 153: 1037-1042.
[21] Blue R, Li C, Spadola M, Saylany A, McShane B and Lee JYK. Complication rates during endoscopic microvascular decompression surgery are low with or without petrosal vein sacrifice. World Neurosurg 2020; 138: e420-e425.
[22] Cheng L, Guo P, Liao YW, Zhang HL, Li HT and Yuan X. Pathophysiological changes in the cerebellum and brain stem in a rabbit model after superior petrosal vein sacrifice. Biosci Rep 2018; 38: BSR20171043.
[23] Eibach S, Steinfort B and Di Ieva A. Delayed contralateral trigeminal neuralgia after microvascular decompression and postoperative changes in venous outflow. World Neurosurg 2020; 140: 107-108.
[24] Liebelt BD, Barber SM, Desai VR, Harper R, Zhang J, Parrish R, Baskin DS, Trask T and Britz GW. Superior petrosal vein sacrifice during microvascular decompression: perioperative complication rates and comparison with venous preservation. World Neurosurg 2017; 104: 788-794.
[25] Inoue T, Hirai H, Shima A, Suzuki F, Fukushima T and Matsuda M. Diagnosis and management for trigeminal neuralgia caused solely by venous compression. Acta Neurochir (Wien) 2017; 159: 681-688.
[26] Xiong NX, Zhou X, Yang B, Wang L, Fu P, Yu H, Wang Q, Abdelmaksoud A, Yuan Y, Liu W, Huang Y, Budrytė K, Huang T and Zheng X. Preoperative MRI evaluation of relationship between trigeminal nerve and superior petrosal vein: its role in treating trigeminal neuralgia. J Neurol Surg A Cent Eur Neurosurg 2019; 80: 213-219.